CHANGES IN THE SARCOPLASMIC RETICULUM MEMBRANE PROFILE INDUCED BY ENZYME PHOSPHORYLATION TO $E_1 \sim P$ AT 16 Å RESOLUTION VIA TIME-RESOLVED X-RAY DIFFRACTION

D. PASCOLINI,* L. G. HERBETTE,‡ V. SKITA,* F. ASTURIAS,* A. SCARPA,§ AND J. K. BLASIE*
*Department of Chemistry, Unversity of Pennsylvania, Philadelphia, Pennsylvania 19104;
‡Departments of Radiology, Medicine and Biochemistry, University of Connecticut, Farmington, Connecticut 06032; §Department of Biochemistry/Biophysics, University of Pennsylvania, Philadelphia, Pennsylvania 19104

ABSTRACT Time-resolved x-ray diffraction studies of the isolated sarcoplasmic reticulum (SR) membrane have provided the difference electron density profile for the SR membrane for which the Ca^{2+}ATPase is transiently trapped exclusively in the first phosphorylated intermediate state, $E_1 \sim P$, in absence of detectable enzyme turnover *vs.* that before ATP-initiated phosphorylation of the enzyme. These diffraction studies, which utilized the flash-photolysis of caged ATP, were performed at temperatures between 0 and −2°C and with a time-resolution of 2–5 s. Analogous time-resolved x-ray diffraction studies of the SR membrane at 7–8°C with a time resolution of 0.2–0.5 s have previously provided the difference electron density profile for the SR membrane for which the Ca^{2+}ATPase is only predominately in the first phosphorylated intermediate state under conditions of enzyme turnover vs. that before enzyme phosphorylation. The two difference profiles, compared at the same low resolution (~40 Å), are qualitatively similar but nevertheless contain some distinctly different features and have therefore been analyzed via a step-function model analysis. This analysis was based on the refined step-function models for the two different electron density profiles obtained independently from x-ray diffraction studies at higher resolution (16–17 Å) of the SR membrane before enzyme phosphorylation at 7.5 and −2°C. The step-function model analysis indicated that the low resolution difference profiles derived from both time-resolved x-ray diffraction experiments arise from a net movement of Ca^{2+}ATPase protein mass from the outer monolayer to the inner monolayer of the SR membrane lipid bilayer. The conserved redistribution of this protein mass is however somewhat different for the two cases, especially at the extravesicular membrane surface containing the Ca^{2+}ATPase "headpiece." However, the conserved redistribution of protein mass within the SR membrane lipid bilayer common to both cases is clearly due to $E_1 \sim P$ formation.

INTRODUCTION

The ATP-driven active transport of calcium across the sarcoplasmic reticulum (SR) membrane profile by the integral membrane protein Ca^{2+}ATPase is generally thought to involve a cyclical sequence of partial reactions. The sequence includes distinct chemical intermediate states of the Ca^{2+}ATPase enzyme and an alternation between two major distinct conformational states, E_1 and E_2 (1–3).

We have previously studied the kinetics of ATP-induced Ca^{2+} uptake as a function of temperature between 26 and −2°C in vesicular dispersions and oriented multilayers of isolated SR membranes (4, 5). These studies utilized double-beam spectrophotometric techniques and the metallochromic indicator arsenazo III to detect the calcium transport process and the flash photolysis of caged ATP (6) to synchronously initiate the calcium transport cycle among the ensemble of the Ca^{2+}ATPase molecules. At least two phases in the uptake kinetics were detected: a fast phase identified with calcium "occlusion" and the formation of the ADP-sensitive, acid-stable phosphorylated intermediate state of the enzyme, $E_1 \sim P$, and a slow phase identified with calcium translocation across the membrane profile after the conversion of the enzyme to the E_2 conformation and subsequent turnover of the enzyme. The transport kinetics have a strong temperature dependence (4, 5): the slow phase, which at 10–25°C appears within only a few hundred milliseconds into the fast phase, at lower temperatures, below 5–7°C, appears with considerable delay of several seconds well into the plateau of the

A. Scarpa's present address is Department of Physiology and Biophysics, Case Western University, Cleveland, OH 44106.

V. Skita's present address is Biomolecular Structure Analysis Center, University of Connecticut Health Center, Farmington, CT 06032.

fast phase. This delay is most clearly demonstrated in the results of the calcium uptake kinetics in oriented multilayers of SR membranes at 0 and −2°C shown in Fig. 1, and ranges from ~6 s at 0°C to ~8 s at −2°C. (The results in Fig. 1 represent a minor extension of our previous studies and were obtained utilizing the Hg-arc for the flash-photolysis with all other experimental conditions as in reference 5). Because the fast phase is identified with the formation of the first phosphorylated intermediate $E_1 \sim P$, the delay in the onset of the slow phase, identified with Ca^{2+} translocation requiring the conversion of $E_1 \sim P$ to $E_2 \sim P$, must represent, according to the scheme of de Meis and Vianna (1), an extension of the lifetime or a "transient trapping" of the first phosphorylated intermediate.

This transient trapping of the first phosphorylated intermediate of the Ca^{2+}ATPase appears to originate from a structural change of the SR membrane. At a characteristic temperature of 2–3°C we have reported a reversible, temperature-induced structural transition for the SR membrane profile, which involves lipid lateral phase separation in the plane of the membrane and a corresponding redistribution of Ca^{2+}ATPase protein mass from the inner monolayer of the membrane lipid bilayer to the outer monolayer and to the extravesicular surface of the membrane, as described in detail in reference 7. Because the transient trapping of $E_1 \sim P$ is in this case mediated only by decreasing the temperature below this transition, it appears that the structural changes in the lipid and protein components of the membrane are responsible for the increased lifetime (transient trapping) of the intermediate.

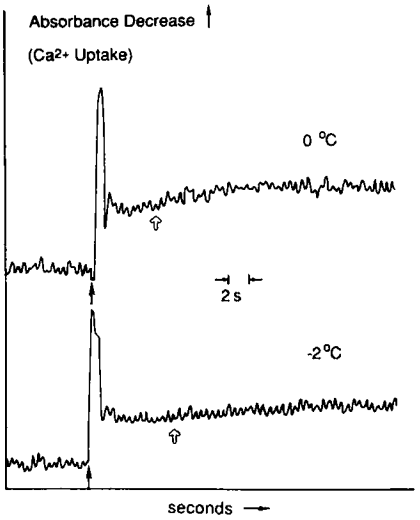

FIGURE 1 Calcium uptake kinetics of oriented SR membrane multilayers at 0 and −2°C, monitored spectrophotometrically using the metallochromic dye arsenazo III. Calcium transport was initiated synchronously for the Ca^{2+}ATPase molecules in the multilayer via the flash-photolysis of caged ATP utilizing an UV light flash of ~700 ms from a Hg-arc; the beginning of the UV flash is indicated by the solid arrow, the large peak immediately after is a flash artifact. All experimental conditions are the same as for previous experiments (5). Multilayers were prepared by sedimenting 1 mg of SR protein from a solution of 40 mM Tris maleate, 8 mM $MgCl_2$, 120 mM KCl, 50 μM arsenazo III, 1.75 mM glutathione, 25 μM $CaCl_2$; 200 nmol of caged ATP were added to the multilayer surface. More experimental details and a discussion of the Ca^{2+} calibration are given in reference 5. Both kinetic phases of calcium uptake occurring at higher temperatures are also observed under these lower temperature conditions, but the slow phase does not appear until ~6 s into the plateau of the fast phase at 0°C and until ~8 s at −2°C, as indicated by the open arrows. Multilayers containing caged ADP or no nucleotide served as controls (5) and in such experiments no significant decrease in absorbance was observed.

The calcium uptake kinetics studies and the structural studies for the SR membrane below the structural transition discussed above have provided the basis for time-resolved structural studies of the SR membrane reported herein for which the Ca^{2+}ATPase is transiently trapped exclusively in the intermediate state $E_1 \sim P$ of the enzyme. Such time-resolved x-ray diffraction studies have previously (8) been successful in providing the profile structure for the Ca^{2+}ATPase molecule itself in only predominately the first phosphorylated intermediate state under conditions of enzyme turnover, that is for the SR membrane at 7–8°C and with a time-resolution of 0.2–0.5 s. The time-resolved x-ray diffraction studies at 0 to −2°C presented in this paper have substantially the same nature as the previous time-resolved studies at 7–8°C (8): the overall Ca^{2+} transport process is initiated synchronously for the ensemble of the Ca^{2+}ATPase protein molecules in the oriented multilayer via the flash photolysis of caged ATP; lamellar x-ray diffraction is recorded from the multilayer before the flash-photolysis and immediately after the flash-photolysis; the exposure time for the lamellar diffraction is chosen to be shorter than the lifetime of the trapped intermediate $E_1 \sim P$. The diffraction patterns are analyzed to detect changes within the profile structure of the SR membrane which, given the time resolution of the experiment, can be correlated with the structure of the transiently trapped $E_1 \sim P$ intermediate.

Because the profiles so obtained are at relatively low resolution, they have been subjected to a step-function model analysis to interpret the structural changes within them. Such model analysis utilized the refined step-function model for the SR membrane under low temperature conditions derived independently at a higher resolution of ~17 Å (7). The same step-function model analysis has, for comparative purposes, been applied independently to the profiles from the previous time-resolved x-ray diffraction studies at 7–8°C utilizing the refined step-function model for the SR membrane at 7.5°C derived at ~16 Å resolution in the same study as for the SR membrane at −2°C (7). Previous model analysis of these time-resolved data at 7–8°C (8) were based on the independent knowledge of the separate protein profile structure at 7–8°C. This step-function model analysis for the two time-resolved studies allowed a direct comparison of the

structural changes in the profile for the SR membrane for which the Ca^{2+}ATPase is only predominately in the first phosphorylated intermediate state of the enzyme under conditions of enzyme turnover (7–8°C) with the structural changes in the profile for the SR membrane for which E_1~P is transiently trapped in the absence of detectable enzyme turnover.

This study has been reported previously in abstract form (9).

METHODS

Oriented multilayers of isolated, highly purified SR membranes, containing caged ATP or caged ADP to produce a final caged substrate/Ca^{2+}ATPase mole ratio of 1:2 in the multilayer after partial dehydration were prepared as described previously (10, 11). The multilayers were partially dehydrated at temperatures ranging from 0 to −2°C and maintained at these temperatures throughout the time-resolved x-ray diffraction experiment. The partially dehydrated multilayers were maintained at a constant humidity by placing a saturated salt solution in the sealed canisters containing the multilayers, as previously described (8). The flash photolysis of the caged substrates was obtained using a UV light pulse of the duration of 1 s from a filtered Hg-arc (300–370 nm), delivered to the multilayer via a quartz light guide (5). The time-resolved x-ray diffraction experiments utilized focused, monochromatic (8,980 eV) synchrotron radiation from a wiggler-magnet beam line (12) at the Stanford Synchrotron Radiation Laboratory, Stanford, CA, and the diffraction was recorded with a SIT (silicon intensified target) two-dimensional detector (13). Details on the instrumentation and the diffraction geometry have been given previously (8).

The time-resolved x-ray diffraction experiment consisted of a series of consecutive x-ray exposures of identical length (ranging from 2 to 5 s) from the same multilayer, with three exposures before the UV flash-photolysis of the caged substrate, three following the UV flash and three 5 min after the UV flash. The first exposure after the UV flash was timed to start with a delay $\tau = 0$ s with respect to the UV flash. A delay of ~17 s, intrinsic to the read-out cycle of the SIT detector, occurred between each exposure in the series.

The two-dimensional lamellar diffraction patterns recorded with the SIT detector were angularly integrated over the small mosaic spread exhibited by these oriented multilayers to produce one-dimensional intensity functions $I(z^*)$, with $z^* = 2 \sin\theta/\lambda$, as discussed previously (8). All the diffraction patterns in each series were so integrated using identical integration parameters. To compare quantitatively the diffraction patterns recorded before the UV flash with the patterns following the UV flash, the one-dimensional intensity functions $I(z^*)$, inclusive of the background, were divided in four contiguous regions of z^* each containing one of the four Bragg diffraction maxima (as indicated in Fig. 2) and the integrated areas of these maxima were calculated for each intensity function in an exposure sequence. Because it was always found that the two patterns immediately before the UV flash did not exhibit any significant evolution of the sample nor any instabilities of the incident beam and/or the SIT detector, an average integrated intensity (and standard deviation) was calculated for each of the four diffraction maxima of $I(z^*)$ over these two patterns before the UV flash. Differences were then calculated between the integrated intensities of corresponding diffraction maxima in each pair of successive $I(z^*)$ functions in the same exposure sequence and were expressed as a plus/minus percentage difference with respect to their average integrated values before the UV flash.

The correct electron density profiles for the SR membrane pair within the multilayer unit cell were calculated using the Generalized Fourier Synthesis Deconvolution Method (GFSDM [14]) and the continuous lamellar intensity functions from four experiments utilizing caged ATP.

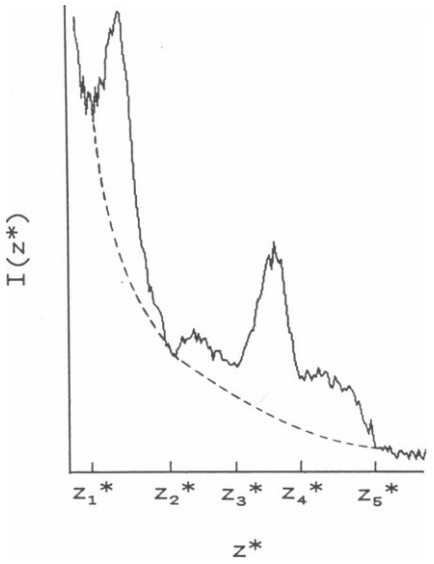

FIGURE 2 Typical lamellar (meridional) x-ray diffraction pattern for an oriented SR membrane multilayer containing caged ATP for a time-resolved diffraction experiment at 0°C and with a time resolution of 5 s. The pattern was recorded before the UV flash photolysis. The intensity function $I(z^*)$ is obtained upon angular integration over the mosaic spread of the two-dimensional diffraction pattern recorded on a SIT detector and contains four maxima corresponding to the first four orders of lamellar diffraction for a disordered multilayer lattice with periodicity $d \sim 193$ Å. The z^*-positions $z_1^* \ldots z_5^*$ indicated refer to integration windows employed in the analysis of the time-resolved data (see Methods). The dotted line represents the estimated lamellar background scattering function taken to be the same for all exposures in a time-resolved experimental exposure sequence.

These four experiments were selected based on the analysis of the integrated intensities for the four Bragg diffraction maxima described above (see Results). Before analysis by the GFSDM, the intensity functions were corrected by an estimated lamellar background scattering function and by a further correction proportional to z^*, allowing for the cylindrical curvature of the multilayers, as previously described (7). These low-resolution (~40 Å) unit cell electron density profiles were then subjected to a model refinement analysis that utilized the step-function model at higher resolution (16–17 Å) calculated previously for oriented SR membrane multilayers under such low-temperature conditions (7).

RESULTS

Fig. 2 shows a lamellar x-ray diffraction pattern from an oriented SR membrane multilayer containing caged ATP, belonging to a sequence of patterns constituting a typical time-resolved x-ray diffraction experiment at ~0°C (see Methods for a description of these sequences). The pattern shown was recorded immediately before the flash-photolysis and the exposure time, identical for all patterns in the sequence, was 5 s. The one-dimensional lamellar intensity function $I(z^*)$ displayed, obtained upon angular integration over the mosaic spread of the two-dimensional pattern recorded on the SIT detector, is characteristic of an oriented SR membrane multilayer partially dehydrated and maintained at ~0°C, that is, below the structural transition observed for the SR membrane profile at ~2°C

(see reference 7 for details on the nature of this transition).[1] The intensity function $I(z^*)$ is typical of all the patterns obtained in these time-resolved x-ray diffraction experiments at 0 to −2°C. It contains four maxima corresponding to the expected positions of the first four Bragg orders of lamellar diffraction from a disordered multilayer lattice with periodicity $d \sim 193$ Å.

To determine if the changes in the lamellar x-ray diffraction patterns after the UV flash photolysis of the caged ATP in the multilayer with respect to the patterns before the flash are statistically significant, the patterns before the flash and the patterns after the flash in each sequence were quantitatively compared in terms of the integrated intensities of the four diffraction maxima in $I(z^*)$ (see Methods). This analysis of the differences between the integrated intensities of corresponding diffraction maxima in successive patterns indicated that an increase, of different extent for each maximum, occurred in the integrated intensities of all four maxima only for the pattern immediately after the UV flash. This increase, expressed as a percentage difference with respect to their average integrated value before the UV flash, was significantly larger than the percentage error expected for that integrated intensity based on the patterns before the UV flash. Following is a typical set of results: the first value is the difference between the integrated intensity of a diffraction maximum in the pattern immediately after the flash and the corresponding maximum in the pattern immediately before the flash, expressed as a percentage of the average integrated intensity for that maximum before the flash; the second value is the expected percentage error for the integrated intensity of that maximum.

First order maximum	+1.59	±0.21
Second order maximum	+4.94	±1.83
Third order maximum	+2.15	±0.54
Fourth order maximum	+5.88	±0.20

These values were in fact similar for eight of the nine time-resolved experiments utilizing caged ATP. Four of these eight time-resolved experiments were selected for further analysis (see below) based on the smaller percentage errors so determined. Control experiments utilized multilayers containing caged ADP or no nucleotide and otherwise identical experimental conditions as for multilayers containing caged ATP. The same analysis of the percentage differences between the corresponding four diffraction maxima in successive exposures before and after the UV flash did not detect such an increase in the integrated intensities of any of the diffraction maxima after the UV flash, but rather indicated either no change or a decrease of similar extent in the integrated intensity of each maximum throughout the exposure sequence. The one atypical experiment employing caged ATP (see above) behaved as these controls (see reference 8 for a discussion of such atypical behavior).

The four time-resolved experiments with the smallest errors (see above) were further analyzed as follows: the continuous lamellar intensity functions $I(z^*)$ recorded immediately before the UV flash and immediately after the UV flash in the same sequence were corrected by the same estimated lamellar background scattering function and by a further correction proportional to z^*, due to the cylindrical curvature of the multilayers (10, 15), and subjected to the GFSDM analysis (14). This analysis has provided the typical low (~40 Å) resolution until cell electron density profiles $\rho_{exp}(z)$ in Fig. 3, consistent with the profiles at similar resolution obtained separately for oriented multilayers of SR membranes under low temperature conditions (Fig. 9 *B* of reference 7). Note that the low-resolution, centrosymmetric unit cell profiles $\rho_{exp}(z)$ contain two apposed single membrane profiles (each single membrane within $0 \leq |z| \leq 96.5$ Å for the solid line and within $0 \leq |z| \leq 98$ Å for the dashed line) and are representative of the two apposed membranes of a collapsed unilamellar vesicle. The unit cell electron density profile for the SR membrane immediately before the UV flash, $\rho_{exp}(z)$, the solid line, is significantly different from that for the SR membrane immediately after the UV flash, $\rho'_{exp}(z)$, the dashed line, upon photolysis of the caged ATP. The differences in these profiles are clearly experimentally significant based on the analysis of the corresponding

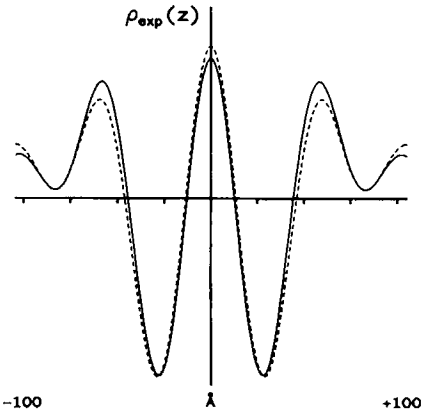

FIGURE 3 Unit cell electron density profiles at low resolution (~40 Å) calculated from phased lamellar intensity functions for the SR membrane multilayer immediately before the UV flash photolysis and caged ATP ($\rho_{exp}[z]$, *solid line*) and immediately after the UV flash ($\rho'_{exp}[z]$, *dashed line*). The differences between the two profiles are experimentally significant (see text). The unit cell profiles extend from $-d/2$ to $d/2$ with a single membrane profile containd within $0 \leq |z| \leq 96.5$ Å for $\rho_{exp}(z)$ and within $0 \leq |z| \leq 98$ Å for $\rho'_{exp}(z)$. Abscissa in Figs. 3–6 is the real space coordinate z; one division equals 25 Å.

[1]The lattice periodicity for these multilayers containing caged ATP differs from the lattice periodicity for the multilayers in reference 7, i.e., 193 Å vs. 211 Å. As a consequence of this change in the lattice, the relative intensities of the reflections in Fig. 2 are slightly different than in Fig. 1 *C* of reference 7.

differences in the integrated intensities of the four lamellar diffraction orders as described above. These differences include an increase of lattice periodicity of ~3 Å, a shift of ~2 Å for the maximal at $|z| \sim 60$ Å and of ~1 Å for the minima at $|z| \sim 28$ Å, a redistribution of electron density throughout the low resolution profile, with, in particular, a loss of density at $|z| \sim 0$ Å and increase of density at $|z| \sim 60$ Å, upon photolysis of caged ATP in the SR membrane multilayer.

STEP-FUNCTION MODEL ANALYSIS

The unit cell electron density profiles $\rho_{exp}(z)$ and $\rho'_{exp}(z)$ in Fig. 3, while clearly indicating that changes occur in the structure of the SR membrane profile after the UV flash-photolysis of the caged ATP, do not illustrate the origin of these changes in terms of the membrane's molecular components primarily because of the inherent low resolution of the profiles. A step-function model analysis, based on the refined step-function model profile obtained separately at higher resolution (~17 Å) for the SR membrane profile under similar low-temperature conditions, has therefore been utilized to interpret the differences between the two profiles in Fig. 3. This step-function model profile (Fig. 10 *C* in reference 7 and the solid line in Fig. 4) had been refined to the unit cell electron density profile at ~17 Å resolution containing the membrane pair, derived for oriented SR membrane multilayers prepared as the multilayers utilized in the time-resolved x-ray diffraction experiments, that is, partially dehydrated and maintained at 0 to −2°C, with the only difference that they did not contain caged ATP. The steps of uniform electron density within this step-function model profile could be identified with the various membrane molecular components following our previous interpretation of the SR membrane profile (16) at this higher resolution as described in detail in reference 7. The following procedure was utilized for the step-function model analysis applied to these time-resolved x-ray diffraction experiments.

(*a*) The step-function model profile at 17 Å resolution, adopted directly from reference 7, was Fourier transformed to obtain a "model" unit cell structure factor calculated to $z^* \sim 1/17$ Å^{-1}; (*b*) this model structure factor was truncated at the same resolution as the time-resolved x-ray diffraction experiment, namely $z^* \sim 1/40$ Å; (*c*) the Fourier transform of the truncated model structure factor is a continuous electron density profile at low resolution, $\rho_{mod}(z)$, which corresponds to the experimental profile $\rho_{exp}(z)$ for the SR membrane before the UV flash, the solid line in Fig. 3; (*d*) the magnitudes of the uniform electron density levels of the steps within the step-function model at 17 Å resolution were modified arbitrarily to predict a 17 Å resolution step-function model for the SR membrane profile after the UV flash. (These modifications were such that the average electron density of the unit cell was conserved and did not alter the widths

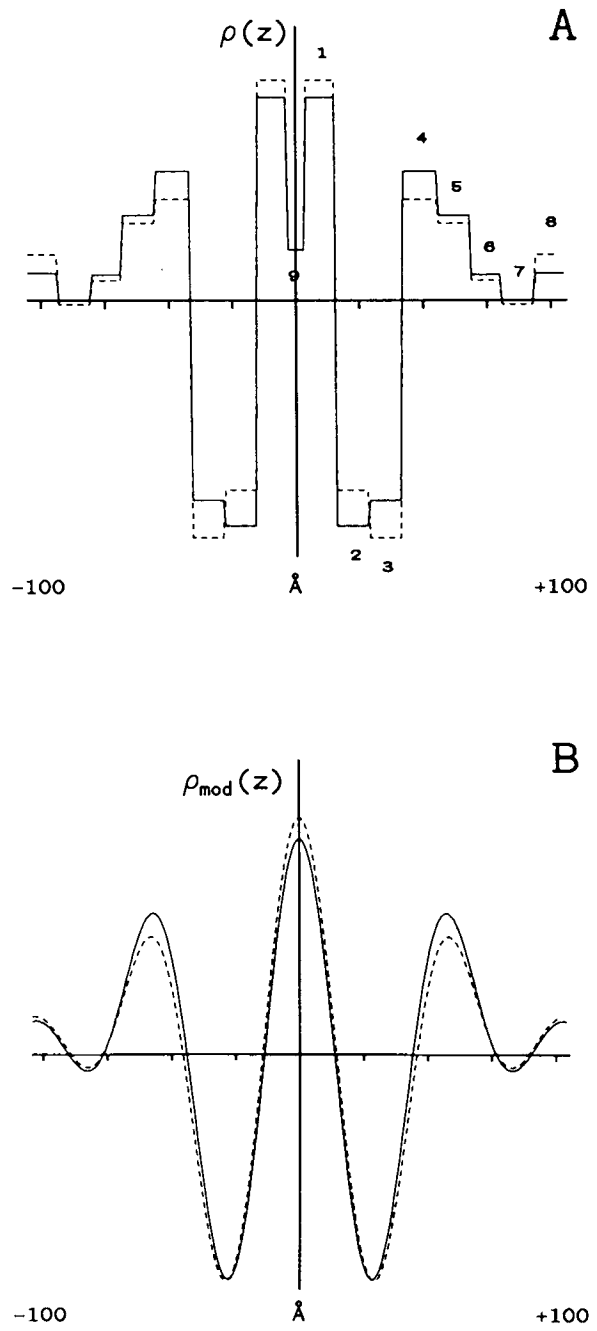

FIGURE 4 Results of the step-function model analysis applied to the time-resolved x-ray diffraction experiments performed at 0 to −2°C and with a time resolution of 2–5 s. (*A*) The solid line is the step-function model profile at moderate resolution (17 Å) for the SR membrane pair immediately before the UV flash photolysis of the caged ATP in the multilayer; the dashed line is the step-function model which best predicts $\rho'_{exp}(z)$ in Fig. 3. See the text for a discussion of the differences between the two step-function model profiles. According to our previous interpretation of the moderate resolution step-function model, relative to a single membrane profile the numbers indicate the following regions of the membrane profile: 1 and 4, the lipid polar headgroup regions of the inner and outer monolayer, respectively; 2 and 3, the lipid fatty acyl chain region of the inner and outer monolayer, respectively; 5–8, the extravesicular surface of the membrane (outside the lipid bilayer) containing the Ca^{2+}ATPase "headpiece"; 9, the intravesicular water space. (*B*) Electron density profiles at low resolution (~40 Å) obtained from the pair of step-function model profiles in *A*. $\rho_{mod}(z)$ is the solid line, $\rho'_{mod}(z)$ is the dashed line; these profiles and their differences agree with the experimental electron density profiles in Fig. 3 at the same resolution.

of the steps.) (*e*) Operations *a* and *b* are repeated on these so-modified step-function models to obtain a continuous electron density profile, $\rho'_{mod}(z)$, at low resolution, to be compared with the experimental profile $\rho'_{exp}(z)$ for the SR membrane after the UV flash, that is, the dashed line in Fig. 3. (*f*) Operations *d* and *e* were then iterated exhaustively to obtain the 17 Å resolution step-function model that best predicts $\rho'_{exp}(z)$.

The results of this step-function model analysis are shown in Fig. 4. In *A* the solid line is the step-function model profile at moderate resolution for the SR membrane before the UV flash-photolysis; changes within this step-function model have been introduced to obtain the step-function model profile (dashed line) which best predicts the low resolution electron density profile for the SR membrane after the UV flash. The changes, relative to a single-membrane profile, include a decrease of density for steps 3 and 4 and a corresponding gain of density for steps 1 and 2. Only a very small change of density occurs for steps 5–8. According to our previous interpretation of the moderate resolution step-function model profile, these changes correspond to conserved redistribution of electron density from the phospholipid headgroup region and acyl chain region of the outer monolayer into the phospholipid headgroup and acyl chain regions of the inner monolayer within the lipid bilayer region of the SR membrane profile. The density on the extravesicular surface of the membrane profile remains virtually unchanged. Taking into account that lipid flip-flop between the two monolayers of the membrane lipid bilayer is much too slow to occur within the time resolution of these time-resolved x-ray diffraction experiments of 2–5 s (16), this redistribution of density must therefore arise from a redistribution of ATPase protein mass, because in these preparations >90% of the protein is Ca^{2+}ATPase (17).

Fig. 4 *B* shows the continous low-resolution electron density profiles obtained from the step-function model profiles in *A*, the solid line is $\rho_{mod}(z)$ and the dashed line is $\rho'_{mod}(z)$. The two low-resolution profiles and the differences between them agree very well with the experimental low-resolution profiles of Fig. 3, except for slightly different values in both functions of the ratios of the maxima at $|z| \sim 0$ and $|z| \sim 60$ Å.[2] A very large number of iterations were attempted in the various modifications of the step-function model profile and it was thereby found that the solution for the step-function model which best predicts $\rho'_{exp}(z)$ seems to be fairly unique in that other modifications within the step-function model simply cannot predict $\rho'_{exp}(z)$. In some cases, these modifications as small as even 2% in the magnitude of only two steps for steps 1–5 with respect to the step-function model profile presented could not predict $\rho'_{exp}(z)$.

An identical step-function model analysis has been applied, for comparative purposes, to data previously obtained from time-resolved x-ray diffraction experiments at 7–8°C with a time-resolution of 0.2–0.5 s (8). For a direct comparison of the results from the step-function model analysis applied to the time-resolved x-ray diffraction experiments at the two temperatures, the lamellar diffraction data from the experiments at 7–8°C have been truncated at the same resolution as the data from the experiments at 0 to −2°C. The experimental unit cell electron density profiles derived at low resolution are shown in Fig. 5, the solid line for the SR membrane immediately before the UV flash photolysis of caged ATP, the dashed line for the SR membrane immediately after the UV flash. In Fig. 6 are shown the results of the step-function model analysis: the step-function model profile for the SR membrane before the UV flash (solid line of Fig. 6 *A*) is the step-function model obtained separately (7) for the SR membrane profile at ~16 Å resolution calculated from the phased lamellar diffraction data from oriented SR membrane multilayers partially dehydrated and in equilibrium at 7.5°C; the oriented multilayers were prepared identically as for the time-resolved experiments, except for the absence of caged ATP. The dashed line in Fig. 6 *A* is the step-function model which best predicts (essentially with uniqueness, as discussed above) the con-

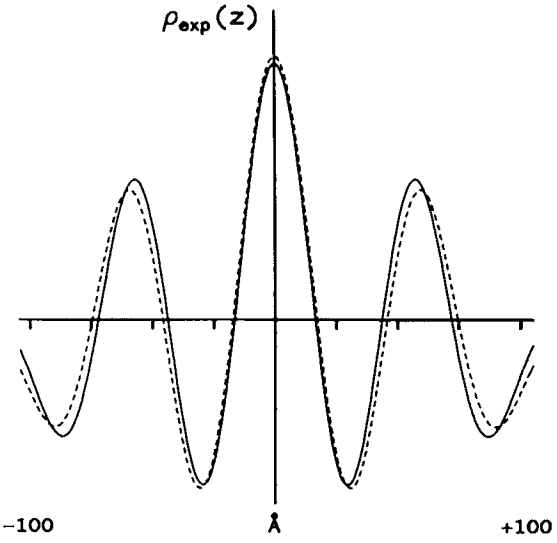

FIGURE 5 Unit cell electron density profiles at low resolution (~40 Å) obtained by truncation of the lamellar diffraction data from previous time-resolved x-ray diffraction studies performed at 7–8°C and with a time resolution of 0.2–0.5 s. The solid line is the electron density profile for the SR membrane pair immediately before the UV flash-photolysis of the caged ATP contained in the multilayer, the dashed line the electron density profile immediately after the flash-photolysis. The unit cell profiles extend from $-d/2$ to $d/2$ with a single membrane contained within $0 \leq |z| \leq 100$ Å.

[2]These small discrepancies exist because in the case of the time-resolved x-ray diffraction experiment, it was possible to integrate over the mosaic spread of the meridional intensity functions due to the use of the area detector. In the case of the experiments under low-temperature conditions at higher resolution, an approximate correction for the mosaic spread was applied to the meridional intensity functions because a linear detector was used.

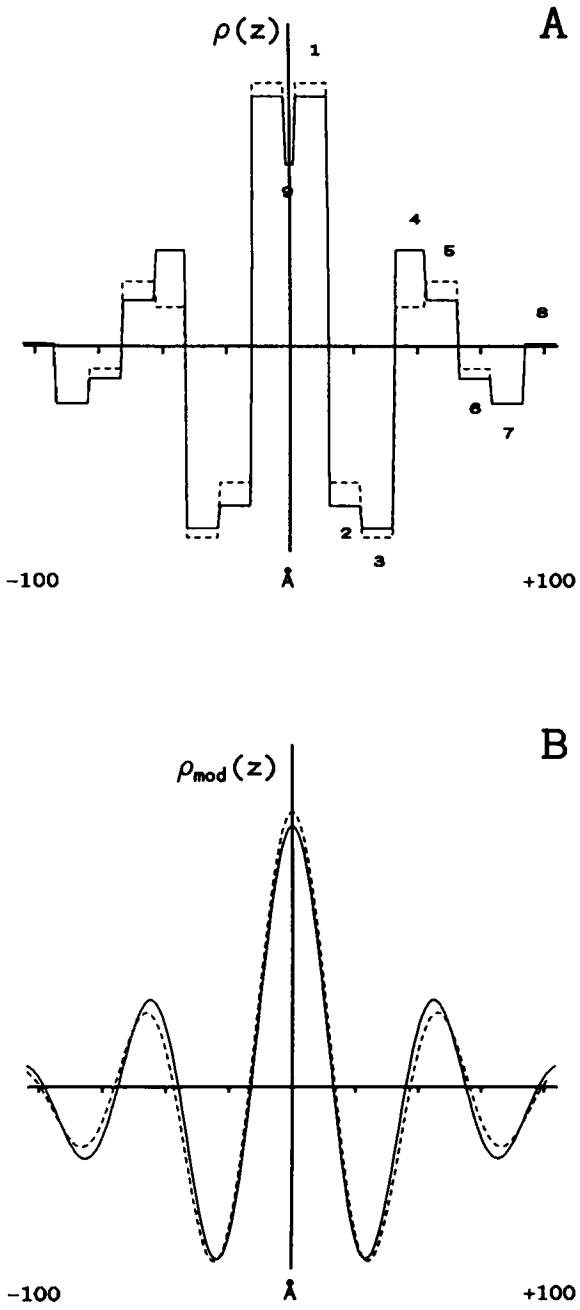

FIGURE 6 Results of the step-function model analysis applied to the time-resolved x-ray diffraction experiments performed at 7–8°C and with a time resolution of 0.2–0.5 s. (*A*) The solid line is the step-function model profile at moderate resolution (16 Å) for the SR membrane immediately before the UV flash-photolysis of the caged ATP in the multilayer; the dashed line the step-function model that predicts best the experimental low resolution electron density profile immediately after the UV flash $\rho'_{exp}(z)$ in Fig. 5. For a discussion of the differences between the two step-function model profiles see the text; for the numbered identification of the steps with the different regions of the membrane profiles see Fig. 4. (*B*) Electron density profiles at low resolution (~40 Å) obtained from the pair of step-function model profiles in *A*. They agree well with the experimental low resolution electron density profiles in Fig. 5 and with the differences between them.

tinuous experimental electron density profile at low resolution $\rho'_{exp}(z)$ for the SR membrane immediately after the flash-photolysis. The continuous low-resolution electron density profiles calculated from the pair of step-function model profiles in Fig. 6 *A* are shown in Fig. 6 *B* and reflect the good fit between the experimental and model electron density profiles. The best step-function model profile for the SR membrane after the UV flash in Fig. 6 *A* indicates, relative to a single membrane profile, a loss of density primarily for step 4 and a corresponding gain of density throughout steps 1, 2, 5, and 6 upon the flash photolysis of caged ATP. Consistent with the interpretation of the step-function model profile given previously (7), electron density is therefore lost mainly in the phospholipid polar headgroup region of the outer monolayer and is gained in part throughout the inner monolayer within the lipid bilayer region within the SR membrane profile and in part on the extravesicular surface of the membrane profile. Again, excluding migration of lipids between the two monolayers of the membrane lipid bilayer on this timescale of 0.2–0.5 s (16), this conserved redistribution of density is identifiable with a redistribution of Ca^{2+} ATPase protein mass within the membrane profile. This result is in agreement with the previous modeling analysis of these time-resolved x-ray diffraction experiments (8) based on the protein profile itself derived independently (16).

DISCUSSION

The time-resolved x-ray diffraction experiments at 0 to −2°C have detected a distinct, significant structural change in the SR membrane profile at low resolution upon photolysis of the caged ATP within oriented SR membrane multilayers. Because this change is not detected in control experiments employing the photolysis of caged ADP under otherwise identical conditions and because the time-scale of the photolysis dark reactions on the order of milliseconds is negligible versus the time-resolution of these time-resolved x-ray diffraction experiments of seconds, this structural change is dependent exclusively upon the appearance of ATP within the multilayer. Moreover, according to the calcium uptake kinetics for SR membrane multilayers at temperatures of 0°C or lower, the Ca^{2+}ATPase intermediate $E_1 \sim P$ is quickly formed and is transiently trapped for significantly longer times relative to the 2–5–s timescale of this time-resolved experiment; therefore the structural change within the SR membrane profile detected within 2–5 s immediately after the UV flash arises exclusively from the transiently trapped intermediate $E_1 \sim P$.

The time-resolved x-ray diffraction studies conducted previously (8) had also detected a structural change in the SR membrane profile occurring within the first turnover of the Ca^{2+}ATPase ensemble and associated unambiguously with the phosphorylation of the Ca^{2+}ATPase protein. The time-resolution (0.2–0.5 s) of these earlier studies was only comparable to or somewhat greater than the expected

lifetime of $E_1 \sim P$ at 7–8°C (18). At low resolution the difference profiles obtained from the two time-resolved experiments appear similar, but not identical. We have compared them using a model refinement analysis which allows the characterization of the structural changes in the electron density profiles at a resolution substantially higher than the experimental resolution. Applied to the difference profile calculated from the time-resolved x-ray diffraction experiments at 0 to −2°C and, independently, to the difference profile from the time-resolved x-ray diffraction experiment at 7–8°C, the model analysis has identified a redistribution of Ca^{2+}ATPase protein mass within the profiles induced by phosphorylation. However, the model analysis also indicates that the conserved redistribution of the protein mass within the membrane profile for which the Ca^{2+}ATPase is only predominately in the first intermediate state of the enzyme under conditions of turnover (7–8°C) is somewhat different than in the membrane profile for which $E_1 \sim P$ is transiently trapped in absence of detectable turnover. The similarity for the two cases (namely a predominant redistribution of protein mass from the outer monolayer into the inner monolayer of the lipid bilayer region in the SR membrane profile) must arise from the formation of $E_1 \sim P$. The differences (namely a redistribution of some minor protein mass from the outer monolayer of the lipid bilayer region onto the extravesicular surface of the membrane profile containing the Ca^{2+}ATPase "headpiece" only for the 7–8°C case) could be explained if either (*a*) for the experiments at 7–8°C, the structural change detected includes changes due to the occurrence of additional structurally distinct intermediates of the Ca^{2+}ATPase within the time resolution of the experiment, or (*b*) if the $E_1 \sim P$ intermediate of the Ca^{2+}ATPase has a distinctly different structure when transiently trapped in absence of turnover. The second possibility may be suggested by the existence of the characteristic structural requirements for the "low temperature" trapping of the $E_1 \sim P$ intermediate described previously (7). However, it must be noted that enzyme turnover still occurs at 0°C or lower temperatures, even if dramatically slower: as a consequence the profile structure of the transiently trapped $E_1 \sim P$ described in this paper remains functionally significant in terms of the Ca^{2+} transport process.

CONCLUSION

These time-resolved x-ray diffraction studies of the SR membrane profile structure reported herein for which the Ca^{2+}ATPase was "transiently trapped" exclusively in the $E_1 \sim P$ intermediate state within the time-resolution of the experiment clearly indicate that the major effect of $E_1 \sim P$ formation involves a conserved redistribution of Ca^{2+}ATPase mass from the outer monolayer to the inner monolayer within the lipid bilayer region of the membrane profile. This result is in agreement with our previous time-resolved x-ray diffraction studies for which the Ca^{2+}ATPase was only predominately in the $E_1 \sim P$ state within the time resolution employed under conditions of enzyme turnover.

This research was supported by a grant from the National Institutes of Health NIH HL-18708 to J. K. Blasie. L. Herbette acknowledges his affiliation as an Established Investigator of the American Heart Association.

Received for publication 25 August 1987 and in final form 13 May 1988.

REFERENCES

1. de Meis, L., and A. L. Vianna. 1979. Energy interconversion by the Ca^{2+}-dependent ATPase of the sarcoplasmic reticulum. *Annu. Rev. Biochem.* 48:275–292.
2. Tanford, C. 1983. Mechanism of free energy coupling in active transport. *Annu. Rev. Biochem.* 52:379–409.
3. Martonosi, A. 1971. The structure and function of sarcoplasmic reticulum membranes. *In* Biomembranes. Vol. 1. L. Manson, editor. Plenum Publishing Corp., New York. 191–256.
4. Pierce, D., A. Scarpa, M. R. Topp, and J. K. Blasie. 1983. Kinetics of calcium uptake by the sarcoplasmic reticulum vesicles using flash photolysis of caged adenosine 5'-triphosphate. *Biochemistry.* 22:5254–5261.
9. Pierce, D., A. Scarpa, D. R. Trentham, M. R. Topp, and J. K. Blasie. 1983. Comparison of the kinetics of calcium transport in vesicular dispersions and oriented multilayers of sarcoplasmic reticulum membranes. *Biophys. J.* 44:365–373.
6. McCray, J. A., L. G. Herbette, T. Kihara, and D. R. Trentham. 1980. A new approach to time-resolved studies of ATP-requiring biological systems: laser flash photolysis of caged ATP. *Proc. Natl. Acad. Sci. USA.* 77:7237–7241.
7. Pascolini, D., and J. K. Blasie. 1988. Moderate resolution profile structure of the sarcoplasmic reticulum membrane under "low" temperature conditions for the transient trapping of $E_1 \sim P$. *Biophys. J.* 54:669–678.
8. Blasie, J. K., L. G. Herbette, D. Pascolini, V. Skita, D. H. Pierce, and A. Scarpa. 1985. Time-resolved x-ray diffraction studies of the sarcoplasmic reticulum membrane during active transport. *Biophys. J.* 48:9–18.
9. Pascolini, D., L. G. Herbette, V. Skita, A. Scarpa, and J. K. Blasie. 1987. Changes in the sarcoplasmic reticulum membrane profile upon $E \sim P$ formation at ~15 Å resolution. *Biophys. J.* 51:346a. (Abstr.)
10. Herbette, L. G., J. Marquardt, A. Scarpa, and J. K. Blasie. 1977. A direct analysis of lamellar x-ray diffraction from hydrated oriented multilayers of fully functional sarcoplasmic reticulum. *Biophys. J.* 20:245–272.
11. Herbette, L. G., A. Scarpa, J. K. Blasie, C. T. Wang, A. Saito, and S. Fleischer. 1981. A comparison of the profile structures of isolated and reconstituted sarcoplasmic reticulum membranes. *Biophys. J.* 36:47–72.
12. Winick, H., and S. Doniach. 1980. Synchrotron Radiation Research. Plenum Publishing Corp., New York. 754 pp.
13. Gruner, S. M., J. R. Milch, and G. T. Reynolds. 1982. Slow-scan silicon-intensified target-TV x-ray detector for quantitative recording of weak x-ray images. *Rev. Sci. Instrum.* 53:1770–1778.
14. Schwartz, S., J. E. Cain, E. A. Dratz, and J. K. Blasie. 1975. An analysis of lamellar x-ray diffraction from disordered membrane multilayers with application to data from retinal rod outer segment. *Biophys. J.* 15:1201–1233.
15. Pascolini, D., J. K. Blasie, and S. M. Gruner. 1984. A 12 Å resolution

x-ray diffraction study of the profile structure of isolated bovine retinal rod outer segment disk membranes. *Biochim. Biophys. Acta.* 777:9–20.

16. Herbette, L. G., P. DeFoor, S. Fleischer, D. Pascolini, A. Scarpa, and J. K. Blasie. 1985. The separate profile structures of the calcium pump protein and the phospholipid bilayer within isolated sarcoplasmic reticulum membranes determined by x-ray and neutron diffraction. *Biochim. Biophys. Acta.* 187:103–122.
17. Meissner, G., G. E. Conner, and J. Fleischer. 1973. Isolation of sarcoplasmic reticulum by zonal centrifugation and purification of Ca^{2+} pump and Ca^{2+} binding proteins. *Biochim. Biophys. Acta.* 298:246–269.
18. Fernandez-Belda, F., M. Kurzmack, and G. Inesi. 1984. A comparative study of calcium transients by isotopic tracer, metallochromic indicator, and intrinsic fluorescence in sarcoplasmic reticulum ATPase. *J. Biol. Chem.* 259:9687–9698.